Dual Resonance Circular Ring-Shaped Metamaterial Absorber with Wide Operating Angle

O. Ayop, M. K. A. Rahim, N. A. Murad, N. A. Samsuri
UTM-Mimos, Faculty of Electrical Enginering, Universiti Teknologi Malaysia, Johor Bahru, Malaysia,
osman@fke.utm.my, mkamal@fke.utm.my, asniza@fke.utm.my, asmawati@fke.utm.my

***Abstract*—This paper proposed a dual resonant circular ring-shaped metamaterial absorber (MMAbs) with wide operating angle in X-band frequency. The structure is constructed on FR4 substrate. The resonating elements are designed using two circular rings structure with different radius. The resonating elements are printed on the top surface of FR4 substrate, while at the bottom layer; a full copper layer is placed. The performance of the designed structure is observed using CST software. From the simulation, the proposed structure achieves high absorbance, which is 93.80% and 86.19% at 9 GHz and 11 GHz respectively for normal incident EM wave. Then, the structure is also simulated for oblique incident angles. It is observed that the operating angle of the proposed metamaterial absorber is 69^{o} for both TE and TM polarization. The measurement is done to validate the simulated result.**

Keywords—dual resonant frequency; wide operating angle; polarization insesnsitive; impedance matching; high absorbance

I. INTRODUCTION

Metamaterial absorbers have received great interest since the first experimental result was proposed by Landy in 2008 [1]. The design consists of ELC resonator with cut wire. With such design, both effective permittivity and permeability can be altered to match the free space impedance. So that, the capability of the structure to absorb the incident of EM wave can be maximized. Using the same principle, many metamaterial absorbers were design to work at single band [2]-[3] and also multi-band [4]-[5]. Many designs of metamaterial absorber do not consider the polarization dependency and found to be unstable at different polarization angle which can limit the application need [6]-[7].

For metamaterial absorber design, the operating bandwidth is always referring to the range of frequency where the absorber can maintain at least 50% of the absorbance magnitude. It is known as full width half maximum (FWHM) bandwidth, where it is normally found between 3% and 5% for each absorbing frequency band [8]-[9]. To improve the bandwidth, a wideband absorber can be designed as presented in [10].

In this paper, a MMAbs with large operating angle is proposed. The structure is designed using circular ring-shaped which is very symmetrical and not sensitive to polarization of incident EM wave. The analysis is done in term of reflectance, transmittance, absorbance, and relative impedance.

II. METAMATERIAL ABSORBER DESIGN

The design of dual resonant circular ring-shaped MMAbs is depicted in Fig. 1. The designed structure consists of two 0.035 mm thick circular rings-shaped copper with different radius printed on 0.8 mm FR4 substrate. The relative permittivity of the dielectric substrate is 4.6 and the loss tangent is 0.019. By proper optimizing the circular ring structure on FR4 substrate, MMAbs with high absorption magnitude can be developed. The radius, r of the circular ring-shaped can be calculated using formula (1).

$$r = \frac{c}{2\pi f_0 \sqrt{\varepsilon_{reff}}} \tag{1}$$

Where; f_0= resonant frequency of the circular ring-shaped and ε_{reff} is the effective relative permittivity of FR4 substrate.

The dual rings-shaped is proposed in order to obtain two resonant frequencies at 9 GHz and 11 GHz. The dimension of the proposed structure is given in Table I. To ease of analysis, the larger circular ring and smaller circular ring are labeled as CR_1 and CR_2 respectively. The dimension of the unit cell ($W \times L \times h$) is approximately $\lambda_g/2 \times \lambda_g/2 \times \lambda_g/20$. The average radius and width of both resonating elements are around $\lambda_g/6$ and $\lambda_g/60$ respectively. The gap between CR_1 and CR_2, g is $\lambda_g/80$. The first resonant is contributed by CR_2 while the higher resonant frequency is contributed by CR_1.

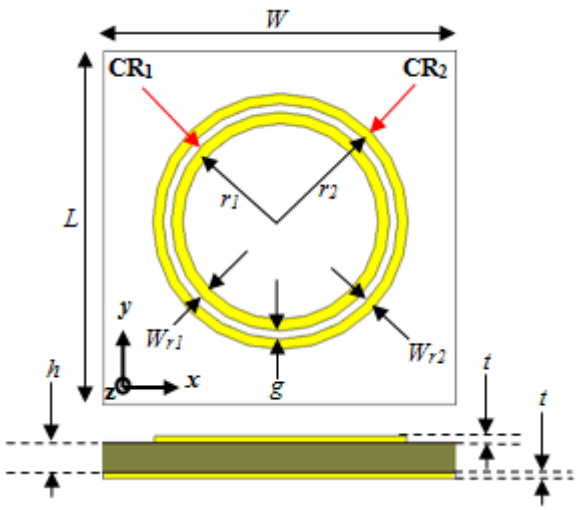

Fig. 1. Unit cell view of dual resonant circular ring shaped MMAbs.

TABLE I. DIMENSION OF DUAL RESONANT CIRCULAR RING-SHAPED MMAbs

Parameters	Dimension (mm)	Dimension in λ_g at resonant
W	9.000	$0.584\lambda_g$
L	9.000	$0.584\lambda_g$
r_1	2.510	$0.163\lambda_g$
r_2	2.975	$0.158\lambda_g$
W_{r1}	0.280	$0.018\lambda_g$
W_{r2}	0.250	$0.016\lambda_g$
g	0.200	$0.013\lambda_g$
h	0.800	$0.052\lambda_g$
t	0.035	$0.002\lambda_g$

III. SIMULATED RESULT

The characteristic of the structure is observed using CST software for normal and oblique incident angle of EM wave. Due to nature of circular ring-shape, which is very symmetrical for all rotating angle, the structure is considered "insensitive" to any polarization angle of incident EM wave. So that, the polarization behavior is not being observed in this work. The simulation is done in unit cell using floquet solver in the simulator.

A. Simulated Transmittance, Reflectance, Absorbance, and Relative Impedance

The simulated reflectance, transmittance, absorbance, and relative impedance of the proposed dual resonant circular ring-shaped MMAbs is illustrated in Fig. 2. The transmittance, T(ω) is zero for all frequency due to the existing of full copper layer at the bottom of the substrate. Hence, the absorbance, A(ω) is determined by reflectance, R(ω) magnitude only using simple formula, A(ω) = 1 − R(ω). For normal incident EM wave, R(ω) are 6.20% and 13.81% so that A(ω) are 93.80% and 86.19% at 9 GHz and 11 GHz respectively. The corresponding FWHM bandwidths are 5.13% (8.74 − 9.20 GHz) and 2.99% (10.88 − 11.21 GHz). The A(ω) at two resonant frequencies are above 86% indicates that high absorbance is achieved.

Next, the simulated relative impedance of the dual resonant circular ring-shaped MMAbs is discussed. At resonant frequency, the relative impedance is given by Z(ω) = 1.0015 + j0.4715 for the first resonant and Z(ω) = 0.5225 − j0.3855 for the second resonant. It shows that at resonant the first resonant frequency, the real part of impedance, Re(Z) is almost unity while the imaginary part of the impedance, Im(Z) is approaching to zero. For the second resonant, the impedance is not achieved unity compared to the first resonant. However, the imaginary part of the second resonant is more approaching zero compared to the first resonant. In can be concluded that impedance matching achieved between the structure of MMAbs and the free space impedance that leads to the high EM wave's absorption especially to the first resonant frequency resulting to the better absorbance magnitude.

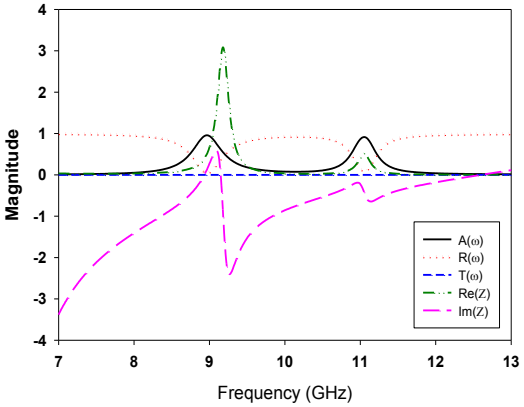

Fig. 2. Graph of simulated reflectance, transmittance, absorbance, and relative impedance.

B. Simulated Absorbance for TE Polarization

Fig. 3 plots the graph of simulated absorbance for TE polarization of incident EM waves. The magnitude of A(ω) for dual resonant circular ring-shaped MMAbs is observed for 20° step angle up to 60°. It is observed that for the first resonant, the A(ω) remain very high up to 60° which is more than 94%. However for the second resonant, the A(ω) decreased to 62.64%. Next, the incident angle is altered until the A(ω) become at least 50%. It is observed that the operating angle for TE mode, θ_{mTE} = 69°. On the other hand, the A(ω) for second resonant decreased rapidly and become around 50% at 69°. Contrarily, the first resonant still manages to achieve A(ω) = 87.27% for the same incident angle. When observing the frequency stability of the MMAbs at resonant for different polarization angle, the first resonant vary between 8.94 GHz and 9.09 GHz (Δf_{r1} = 0.15 GHz). For second resonant, it vary between 10.97 GHz and 11.26 GHz (Δf_{r2} = 0.29 GHz). It shows that the frequency stability is better for lower resonant compared to the higher resonant.

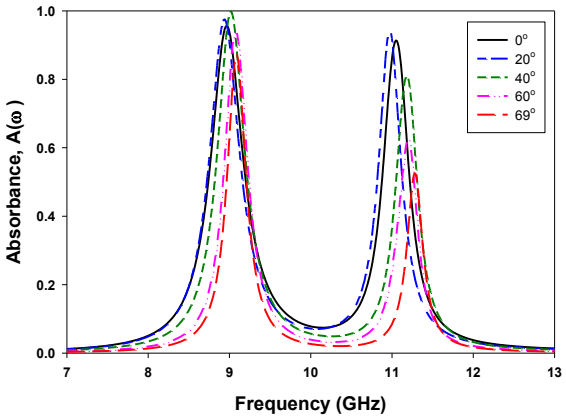

Fig. 3. Graph of simulated absorbance for TE polarization of EM wave.

C. Simulated Absorbance for TM polarization

Next, the simulated absorbance of dual resonant circular ring-shaped MMAbs for TM polarization of incident EM

waves is presented. The result is plotted in Fig. 4. The magnitude of A(ω) is also observed for 20° step angle between 0° and 60°. Similar with TE polarization, the A(ω) remain very high up to 60° which is more than 94%. However for the second resonant, the A(ω) decreased to 62.48%. The operating angle which the A(ω) can maintain at least 50% for TM mode, θ_{mTM} = 69°. It is observed that the A(ω) for second resonant decreased rapidly and become around 50% at 69°. Contrarily, the first resonant still manages to achieve A(ω) = 86.32% for the same incident angle. For TM polarization, the resonant frequency for the first resonant vary between 9.00 GHz and 9.11 GHz (Δf_{r1} = 0.11 GHz) while for second resonant, it vary between 11.03 GHz and 11.24 GHz (Δf_{r2} = 0.21 GHz). It is also proven that the frequency stability is also good for the lower resonant compared to the higher resonant.

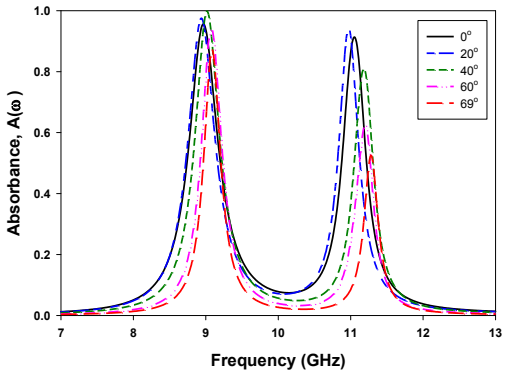

Fig. 4. Graph of simulated absorbance for TM polarization of EM wave.

IV. Measured Result

After optimize the design, the dual resonant circular ring-shaped MMAbs is fabricated on 300 mm × 300 mm FR4 substrate. A total of 1089 unit cells are constructed on the substrate. The photo of the fabricated structure is shown in Fig. 5. The fabricated structure is measured in a special anechoic chamber room using the concept of reflection EM wave between transmitted and received horn antennas. The reflection coefficient of the structure is displayed by network analyzer.

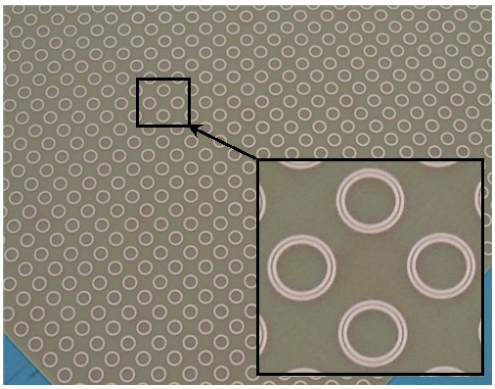

Fig. 5. Fabricated dual resonant circular ring-shaped MMAbs

A. Measured Transmittance, Reflectance, Absorbance, and Relative Impedance

The measured reflectance, transmittance, absorbance, and relative impedance are presented in Fig. 6. As expected, the T(ω) is very small and approaching zero for all measured frequencies. However, the T(ω) is not totally zero due to the size of the fabricated structure which is not infinity. Small signal may pass through the sides around the structure. On the other hand, R(ω) is minimized at two resonance frequencies of 9.42 GHz and 11.60 GHz with magnitude of 1.64% and 9.44% respectively. Hence, A(ω) become 98.36% and 90.56%. The FWHM bandwidths are 5.45% and 3.61% respectively. The measured result verify that the good agreement achieved between simulation and measurement with a frequency shift.

Next, the pattern of characteristic impedance is observed. It can be observed that pattern of graph between simulation (Fig. 2) and measurement (Fig. 6) is in a reasonable agreement. However, the magnitude of imaginary part of the relative impedance, Im(Z) is shifted to higher magnitude for second resonant. At resonant frequency, the relative impedance is given by Z(ω) = 1.222-j0.004 for the first resonant and Z(ω) = 0.8026+j0.6761 for the second resonant. It shows that at the resonant frequency, the real part of impedance, Re(Z) is very close to unity while the imaginary part of the impedance, Im(Z) is almost zero. It is proven that impedance matching achieved between the structures of MMAbs with the free space impedance that leads to the high EM wave's absorption. However, the imaginary part of relative impedance for second resonant is more inductive and will contribute some impedance mismatch. However, the magnitude is still reasonable.

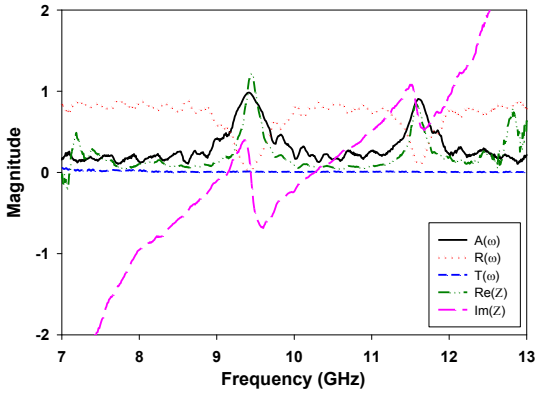

Fig. 6. Graph of measured reflectance, transmittance, absorbance, and relative impedance.

B. Measured Absorbance for TE Polarization

Fig. 7 plots the graph of measured absorbance of the proposed MMAbs for TE polarization. The magnitude of A(ω) is observed for 20° step angle between 0° and 60°. It is observed that the A(ω) remain high up to 60° which is 96.62% for the first resonant and 65.87% for second resonant at 9.44 GHz and 11.62 GHz. There resonant frequency shifted to a little bit higher frequency may be due to fabrication tolerance.

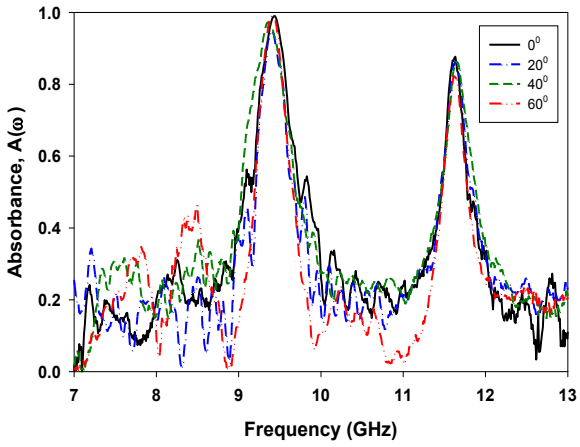

Fig. 7. Graph of measured absorbance for TE polarization incident of EM wave.

C. *Measured Absorbance for TM Polarization*

Fig. 8 plots the graph of measured absorbance of the proposed MMAbs for TM polarization incident EM waves. The observation incident angles are between 0 and 60° with 20° step angle. It is observed that the A(ω) remain very high up to 60° which is more than 99.70% and 82.20% at 9.42 and 11.62 GHz respectively. The measurement is only done up to 60° for both TE and TM polarization because for larger incident angle, high direct coupling between transmitted and received antennas may occur so that the magnitude of absorbance cannot be accurately obtained.

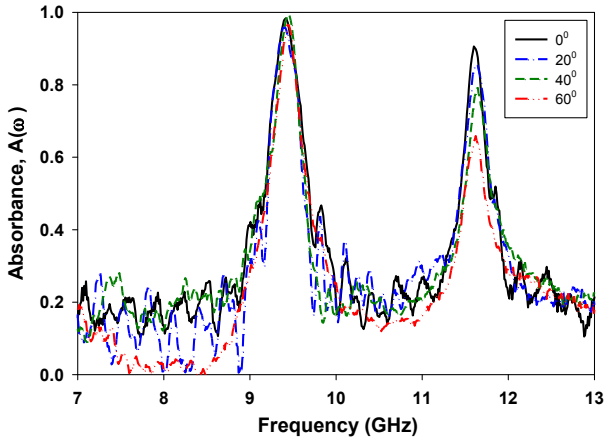

Fig. 8. Graph of measured absorbance for TM polarization of incident EM wave.

Conclusion

In conclusion, this report presents a dual resonant circular ring-shaped MMAbs that is constructed using double circular ring shape printed on FR4 substrate with full ground plane. Due to the symmetrical pattern of the rings, the designed MMAbs is insensitive to the polarizations of the incident wave. The dual band working frequencies, polarization-insensitive and wide operating angle, indicates that the structure can be applied for specific application at X-band frequency.

Acknowledgment

The authors thank the Ministry of Higher Education (MOHE) for supporting the research work, Research Management Centre (RMC), School of Postgraduate (SPS), Communication Engineering Department (COMM) and UTM-Mimos of Universiti Teknologi Malaysia (UTM) and all members of Advanced Microwave lab P18 FKE-UTM for giving motivation, knowledge sharing and support of the research under grant no 4F360/05H35/4L811/4F277.

References

[1] Landy, N. I., S. Sajuyigbe, J. J. Mock, D. R. Smith, and W. J. Padilla, "Perfect metamaterial absorber," Physical Review Letters, Vol. 100, 207402, 2008.

[2] Lei Lu, Shaobo Qu S. Hua Ma, Fei Yu, Song Xia, Zhuo Xu and Peng Bai, "A polarization-independent wide-angle dual directional absorption metamaterial absorber," Progress in Eletromagnetics Research M, Vol. 27, 191-201, 2012.

[3] Yoav Avitzour, Yaroslav A. Urzhumov, and Gennady Shvets, "Wide-angle infrared absorber based on a negative-index plasmonic metamaterial," PHYSIC REVIEW B, vol. 79, 045131, 2009.

[4] L. Huang and H. Chen, "Multi-band and polarization insensitive metamaterial absorber," *Progress In Electromagnetics Research*, Vol. 113, 103-110, 2011.

[5] Qiwei Ye, Yin Liu, Hai Lin, Minhua Li, and Helin Yang, "Multi-band metamaterial absorber made of multi-gap SRRs structure," *Appl Phys A*, Vol. 101, 155-160, 2012.

[6] Gu, S., J. P. Barrett, T. H. Hand, B. I. Popa, and S. A. Cummer, "A broadband low reflection metamaterial absorber," Journal of Applied Physics, Vol. 108, 064913, 2010.

[7] Hu, C., X. Li, Q. Feng, X. N. Chen, and X. Luo, "Introducing dipole-like resonance into magnetic resonance to realize simultaneous drop in transmission and reflection at terahertz frequency," Journal of Applied Physics, Vol. 108, 053103, 2010.

[8] Zhu, B., Z. Wang, C. Huang, Y. Feng, J. Zhao, and T. Jiang, "Polarization insensitive metamaterial absorber with wide incident angle," *Progress In Electromagnetics Research*, Vol. 101, 231-239, 2010.

[9] B. Zhu, C. Huang, Y. Feng, J. Zhao, and T. Jiang, "Dual band switchable metamaterial electromagnetic absorber," *Progress In Electromagnetics Research B*, Vol. 24, 121-129, 2010.

[10] C. Gu, S. Qu, Z. Pei, H. Zhou, and J. Wang, "A wide-band, polarization-insensitive and wide-angle terahertz metamaterial absorber," *Progress In Electromagnetics Research Letters*, Vol. 17, 171-179, 2010.